FEATURE ARTICLE

Photoinduced Cooperative Charge Transfer in Low-Dimensional Organic Crystals

Shin-ya Koshihara,* Yosuke Takahashi, and Hiroyuki Sakai

Department of Applied Physics, Tokyo Institute of Technology, 2-12-1 Oh-okayama, Meguro-ku, Tokyo 152-8551, and Kanagawa Academy of Science and Technology (KAST), KSP Building, 3-2-1 Sakado, Takatsu-ku, Kawasaki 213-0012, Japan

Yoshinori Tokura

Department of Applied Physics, The University of Tokyo, Bunkyo-ku, Tokyo 113, Japan

Tadeusz Luty

Institute of Physical and Theoretical Chemistry, Technical University of Wroclaw, Wybrzeze, Wyspianskiego 27, 50-370, Wroclaw, Poland

Received: October 26, 1998; In Final Form: February 5, 1999

We demonstrate that the cooperative charge transfer among constructive molecules in organic crystals of tetrathiafulvalene-chloranil, i.e., the bidirectional transition between the neutral and ionic phases, can certainly be induced by irradiation of a laser pulse with an 80-fs width. We also report the dynamics of the photoinduced neutral−ionic phase transition by means of the time-resolved spectroscopic technique. Studies using various excitation intensities have shown that the photoconverted fraction (Φ) depends nonlinearly on the excitation intensity. In addition, it has been found that the growth dynamics of the macroscopic domain of the metastable phase strongly depends on the excitation intensity as well. The role of the cooperative charge-transfer interaction in the driving process of this unusual photoeffect is discussed from both the experimental and the theoretical viewpoints.

I. Introduction

A system that shows cooperative phenomena such as a phase transition triggered by external light stimulation is an attractive target for materials science. Recently, it has been reported that weak photoexcitation can trigger macroscopic phase changes in several systems such as π-conjugated polymers, liquid crystals, charge transfer (CT) crystals, radical salts, and transition metal oxides.[1−6] In these materials, cooperative effects in crystals, such as electron−lattice and electron−electron interactions, are considered to play a key role in the driving process of these unusual photoeffects.[7] In other words, the localized photoexcited states and/or photocarriers induce the lattice, electronic, and magnetic structure fluctuations around them via cooperative interactions, finally triggering macroscopic phase changes. In this sense, this effect can be categorized as photoinduced phase transition (PIPT hereafter).

PIPT is an attractive new field for solid state chemistry as well. Structural changes by optical pumping have been extensively studied in the field of photochemistry for many years. However, those studies have been mainly concerned with microscopic reactions confined to one molecule or with local structural changes in crystals. Photoisomerization in the stilbene molecule is a typical example of such a local structural change by photoexcitation. In contrast, the purpose of this study is to report experimental evidence indicating that the local CT excitation induced by the irradiation of ultrashort laser pulses can trigger a change in the valence of a large number of constituent molecules. In other words, the macroscopic phase change between neutral and ionic states can be induced by virtue of cooperative CT interaction, as schematically shown in Figure 1.

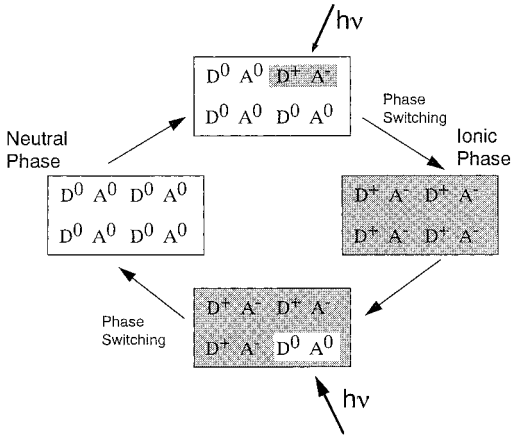

Figure 1. Schematic view graph of the phase change between neutral (D^0A^0) and ionic (D^+A^-) triggered by photoinduced local CT excitation as a result of cooperative CT interaction. Arrows and $h\nu$ denote the photoirradiation for local CT excitation.

We have previously reported that PIPT phenomena show three characteristics because of cooperative interaction.[8,9] The

10.1021/jp984172i CCC: $18.00
Published on Web 03/11/1999

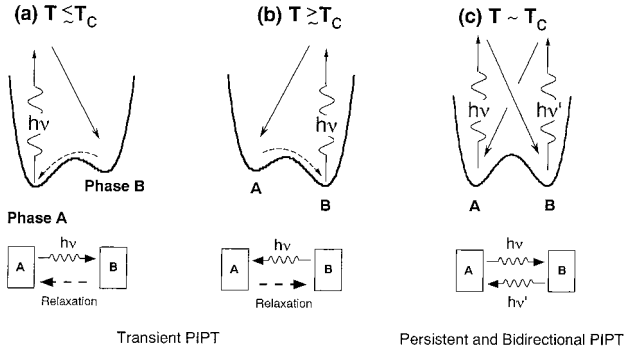

Figure 2. Model free-energy diagrams around the transition temperature T_c for crystals showing the first-order phase transition between A (low-temperature phase) and B (high-temperature phase) phases. Two extreme cases are treated in this figure: (1) The potential barrier between stable and metastable phases is small, and the crystals show the transition without hysteresis or with a narrow one. (2) The potential barrier is too large to induce the phase change thermally between the stable and metastable phases and, as a result, crystals show the phase transition with large hysteresis. (a) and (b) correspond to the former case and (c) to the latter one. Dashed arrows denote the thermally induced relaxation process from the metastable to the stable phase.

first one is the enhancement of the amplitude of photoresponse around the transition temperature (T_c). For example, at the temperature just below T_c, the sample is in the stable phase (A phase) before photoexcitation, as shown in Figure 2a, and the free energy levels of high-temperature (B) and low-temperature (A) phases are nearly degenerate. In this case, even weak photoexcitation can induce a macroscopic phase change from stable (A phase) to metastable (B phase), resulting in a large photoresponse if the metastable phase domain can be generated in the relaxation process after photoexcitation (see Figure 2a).

The second characteristic is that the relaxation dynamics of the photoinjected phase domain depends on the height of the potential barrier in the free energy between two phases. Here, we discuss two extreme cases: (1) The sample shows thermally induced phase transition without hysteresis or with a very narrow one. In other words, the potential barrier between two phases at a temperature close to T_c is rather small, as shown in Figure 2a,b. (2) The sample shows a large hysteresis. In this case, the potential barrier is considered to be too large to induce the change thermally from a metastable phase to a stable one around T_c (see Figure 2c). In the former case (case 1), the photoinjected metastable domain will go back to the original stable one by thermal excitation (see dashed arrows in Figure 2a,b), the PIPT becoming temporal as a result. In fact, the occurrence of a transient PIPT has been reported for several CT crystals, which show a thermally induced phase transition with a narrow hysteresis.[3,5] In contrast, when the potential barrier is large (case 2), the dynamical behavior of the PIPT becomes quite different. At a temperature close to T_c, if the metastable phase domain can be generated in the relaxation process after photoexcitation, the system is considered to be kept in the photogenerated metastable phase rather than the absolutely stable state due to the large energy barrier, as schematically shown in Figure 2c. Therefore, as expected in this case, a permanent and bidirectional PIPT occurred in π-conjugated polymer crystals with large hysteresis width in the thermal phase transition.[1]

The third characteristic of the PIPT is a threshold-like behavior in the excitation intensity dependence of photoconverted fractions (Φ) as observed in π-conjugated polymers.[1,8,9] In the ordinary photoinduced effect, the photoresponse increases parallel to the increase in excitation intensity (see solid line in Figure 3). In contrast, in the case of PIPT, if the excitation-

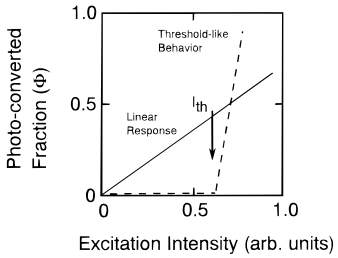

Figure 3. Excitation intensity dependences of the photoconverted fractions (Φ) expected for crystals showing an ordinal photoresponse (solid line) and PIPT (dashed line). The photoinduced signal in an ordinary case, i.e., the photoresponse of the crystals with weak cooperative interaction increases parallel to the increase in excitation intensity. In contrast, the threshold-like behavior as shown by the dashed line is expected for crystals which show PIPT due to strong cooperative interaction.

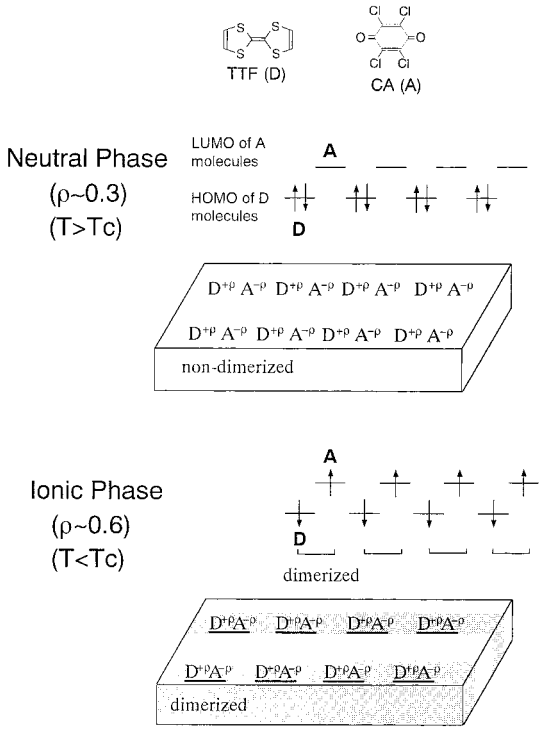

Figure 4. Electronic and structural changes upon the neutral−ionic (N−I) phase transition in TTF-CA crystals. Below T_c, one of the electrons in the highest occupied molecular orbital (HOMO) of the donor moves to the lowest unoccupied molecular orbital (LUMO) of the acceptor. Accompanying changes in the ionicity (ρ) of constituent molecules, the dimerization distortion along the molecular stack axis occurs in the ionic (I) phase.

light intensity becomes stronger than the critical value (I_{th}), the crystal starts the phase transition, which results in a large photoresponse, though the response is very small when the excitation intensity is weaker than I_{th} (see dashed line in Figure 3). It is reasonable to conclude that the existence of a photoexcited species with a density higher than some critical value and/or an unstable phase domain larger than the critical size is necessary to drive the macroscopic phase change from stable to metastable as a thermally induced first-order phase transition.

We will now focus on the PIPT between neutral (N) and ionic (I) phases in organic CT crystals composed of tetrathiafulvalene (TTF) and chloranil (CA). TTF-CA is one of the mixed stack-type CT compounds composed of one-dimensional chains of a donor (D:TTF) and an acceptor (A:CA) (see Figure 4).[10] We report that the cooperative charge transfer among constructive

molecules can be induced in TTF-CA crystals by irradiation of a laser pulse with an 80-fs pulse width, as schematically shown in Figure 1. We also demonstrate that neutral−ionic PIPT (N−I PIPT hereafter) shows the characteristics of photoinduced cooperative phenomena. In chapter VI, we analyze the role of cooperative CT interaction in the driving process of PIPT from a theoretical viewpoint.

II. Experimental Section

Single crystals of TTF-CA with a size of $2 \times 2 \times 3$ mm^3 were prepared by cosublimation of TTF and CA. Constituent compounds were purified by repeated recrystallization and sublimation. Reflectance spectra taken on the (001) surface with light polarization normal to the stack axis (*a* axis) ($E \perp a$) were used for probing the N−I transition. The photoinduced effect was observed by the conventional pump−probe technique using an amplified Ti-sapphire laser pulse. The photon energy of the laser pulse and the pulse width were 1.55 eV and 80 fs, respectively. White light generated by 80-fs pulsed-light irradiation on a 1-mm water cell was used to probe the reflectance change. The pulse width of the white light was approximately 300 fs, and the resolution time of the system was approximately 350 fs. The repetition rate of the amplified Ti-sapphire laser was 1 kHz, but it could be decreased to less than 50 Hz by synchronizing it with a mechanical light chopper.

III. Characteristics of the Neutral−Ionic Phase Transition in TTF-CA Crystals

TTF-CA single crystal is a well-known CT compound located on the neutral−ionic interface.[10] It undergoes the first-order phase transition at ambient pressure accompanying changes in the ionicity of constituent molecules (ρ:D$^{+\rho}$A$^{-\rho}$) (T_c = 81 K, hysteresis width ~2 deg).[10−12] The degree of ionicity, ρ, is relatively high (ca. 0.6) in the low-temperature phase but low (ca. 0.3) in the high-temperature phase. The high-temperature and low-temperature phases are called neutral (N) and ionic (I) phases, respectively. The N−I transition can be classified as a prototypical example of the cooperative valence instability in solids. Figure 4 schematically shows the electronic structural change upon the neutral−ionic (N−I) phase transition. Below T_c, one of the electrons in the highest occupied molecular orbital (HOMO) of the donor moves to the lowest unoccupied molecular orbital (LUMO) of the acceptor. The charged states shown in Figure 4 are schematic. In reality, the estimated value of ρ is fractional (ca. 0.3 in the N-phase and ca. 0.6 in the I-phase) due to the CT interaction (~0.2 eV) between the D and A molecules.[11,13]

The origin of the N−I transition has been attributed to competition between the cost of energy for ionizing D^{0}A^0 stacks and the gain of Madelung energy in the ionic D$^+$A$^-$ lattice.[10,14] Upon the N−I transition, TTF-CA single crystal shows not only a finite jump in ρ but also dimeric lattice distortion in the I-phase (see Figures 4 and 5a,b).[12,13,15] The spin state in the I-phase is analogous to the $S = {}^1/_2$ Heisenberg chain, and the lattice transition is considered to be due to spin-Peierls instability.[16] Such an electron (spin)−lattice interaction obviously plays an important role in promoting N−I transition in real systems in addition to the electrostatic mechanism.[17] Moreover, the dimerization of the lattice in the I-phase breaks the inversion symmetry, and a dielectric response can be expected as a result. Indeed, in the temperature region around T_c, large changes in dielectric constants have been observed (see Figure 5c).[18]

Electron (spin)−lattice interaction and valence instability in this system are expected to become the origin of low-energy

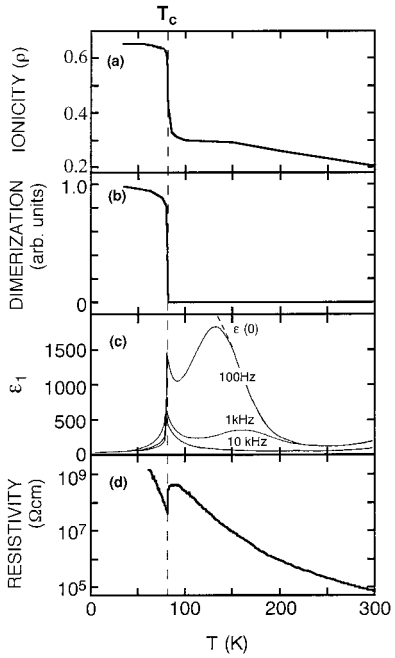

Figure 5. Temperature dependences of various properties of TTF-CA crystals: (a) ionicity (ρ) of the constituent molecules estimated from the frequency of the IR absorption band associated with the C═O stretching mode;[13] (b) degree of the dimeric lattice distortion estimated from the integrated intensity of the (030) neutron diffraction and the (31$\bar{1}$) X-ray diffraction;[12,15] (c) the dielectric constants observed at 0.1, 1, and 10 kHz with the electric field parallel to the *a* axis. The dashed line represents the real part of the static dielectric constant $\epsilon(0)$;[18] (d) resistivity observed with the electric field parallel to the *a* axis. T_c denotes the N−I transition temperature.

excited states such as spin-$^1/_2$ and spin-0 solitons and polarons, as in the case of polyacetylene.[19] Especially in the temperature region around T_c, the energy difference between N- and I-phases becomes small, and hence the neutral−ionic domain wall (NIDW) provides a better picture than solitons and polarons do. These low-energy excited states play an important role as novel characters of this system.[17,18,20−22] For example, the large change in resistivity observed around and below T_c (see Figure 5d) is due to the generation and movement of these low-energy excited states. The theoretical aspects of the N−I transition and the role of low-energy excited species will be discussed in detail in chapter VI.

One of the important characteristics of the N−I transition is large spectral changes that take place in the visible−ultraviolet region. Intramolecular excitation bands of the constituent molecules strongly correlate with their ionicity (ρ:D$^{+\rho}$A$^{-\rho}$).[11] In Figure 6, the reflectance spectra at 77 and 100 K are plotted as an example. Bands B and C are attributed to intramolecular excitations of TTF$^+$ molecules, and band D is attributed to TTF^0 molecules. Therefore, the optical spectra for local electronic excitations can become a very sensitive probe for N−I transition in TTF-CA crystals. We will next use this optical method for probing the N−I transition.

IV. Observation of the Bidirectional Neutral−Ionic Photoinduced Phase Transition (N−I PIPT) in TTF-CA Crystals

The purpose of this chapter is to demonstrate that cooperative valence instability, i.e., phase conversion in both N-to-I and I-to-N directions, can be caused by photoexcitation. Photogenerated CT excitations or resultant charged species locally modify the Coulombic interaction and switch off a channel of

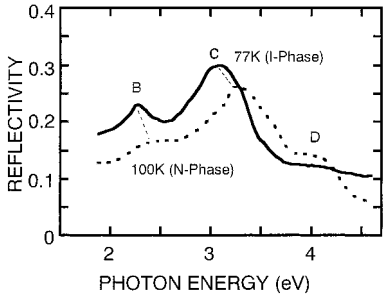

Figure 6. Reflectance spectra of TTF-CA single crystals at 77 K (I-phase: solid line) and 100 K (N-phase: dashed line). The spectra were taken on the (001) surface of the crystal with light polarization normal to the stack axis (*a* axis) ($E \perp a$). Bands B and C are attributed to intramolecular excitations of TTF^{+} molecules, and band D to TTF^{0} molecules.

the collective electron (spin)−lattice interaction. In other words, the generation and movement of NIDW can be triggered by the photoinjected localized species. Therefore, it is reasonable to expect that, if TTF-CA crystals are kept around the critical temperature T_c, even weak and localized photoexcitation could trigger N−I PIPT due to the decreases in difference between the energy levels in the N- and I-phases. In addition, the response to external perturbation will be enhanced due to their low-dimensional structures.

The photoreflectance (PR) spectra in the N- and I-phases, which were measured at 100 and 77 K, respectively, are plotted in Figure 7b,c. PR spectra were recorded as the relative difference ($\Delta R/R$) between the spectra with and without irradiation to the pulsed laser light of 80-fs pulse width. Photoirradiation was made at energies above the CT gap ($h\nu = 1.55$ eV) and nearby the lower energy side of the localized intramolecular excited state of TTF molecules.[11] Solid lines in (b) and (c) indicate the results for well after ($\Delta t = 670$ and 820 ps) pulsed excitation. The photon fluxes for excitation were 5×10^{13} and 4×10^{13} photons/cm^2 (cm^{-2} hereafter) for the observation at 77 and 100 K, respectively. The excitation intensity dependence of the photoconverted fraction will be discussed in the following chapter. Anomalously large PR signals were observed in both I- ((b): 77 K) and N-phases ((c): 100 K). Optimum PR values in the observed photon energy region (between 2 and 3.5 eV) were nearly −0.3 and +0.1 for 77 and 100 K, respectively. It is to be noted that the shape of the PR spectra well after excitation can be reproduced by the calculated differential spectra. In Figure 7a, the differential spectra $\{R(\mathrm{N}) - R(\mathrm{I})\}/R(\mathrm{I})$ and $\{R(\mathrm{I}) - R(\mathrm{N})\}/R(\mathrm{N})$ are plotted by solid and dashed lines. Here, R(N) and R(I) are the typical reflectance spectra in the N- and I-phases shown in Figure 6. The result clearly indicates that the photoexcitations of crystals in the I- and N-phases cause macroscopic I-to-N and N-to-I phase conversions, respectively.

The observed PIPT in the N-to-I direction corresponds to the conversion from the high-temperature phase to the low-temperature phase. Therefore, we can safely conclude that the observed effect is not due to the light-induced heating process across T_c.

The calculated differential spectra plotted in Figure 7a indicate that PR signals at 2.3 eV become approximately −0.3 and +0.4 when the perfect phase conversion in I-to-N and N-to-I directions occurs on the crystal surface. The PR signals observed at the same photon energy (2.3 eV) well after excitation were −0.2 and +0.1 for 77 and 100 K, respectively (see solid lines in Figure 7b,c). It can reasonably be assumed that approximately 65% (=0.2/0.3) and 25% (=0.1/0.4) of the surface of the host

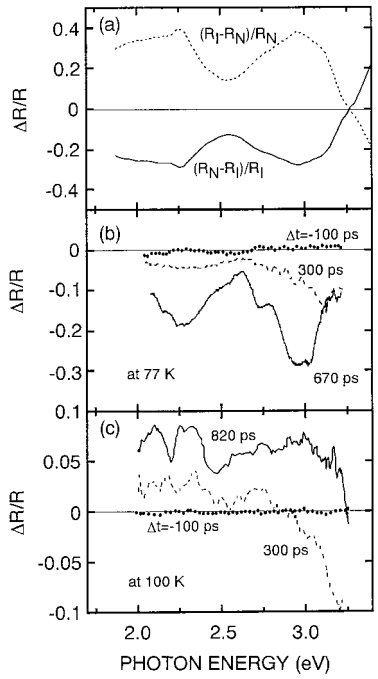

Figure 7. (a) Calculated differential spectra $\{R(\mathrm{N}) - R(\mathrm{I})\}/R(\mathrm{I})$ and $\{R(\mathrm{I}) - R(\mathrm{N})\}/R(\mathrm{N})$ plotted by solid and dashed lines. Here, R(N) and R(I) are the typical reflectance spectra in the N- and I-phases shown in Figure 6. (b) and (c) Time-resolved photoreflectance (PR) spectra in the N- and I-phases, measured at 100 and 77 K, respectively. Δt denotes the interval between the excitation pulse and the white-light pulse for probing reflectance change. Solid, dashed, and dotted lines denote PR spectra observed well after ($\Delta t = 670$ and 820 ps), 300 ps after, and 100 ps before excitation, respectively. PR spectra were recorded as the relative difference ($\Delta R/R$) between the spectra with and without irradiation to a pulsed laser light of 80-fs pulse width. Excitation photon energy was 1.55 eV, and photon flux for excitation was 5×10^{13} and 4×10^{13} cm^2 for observations at 77 and 100 K, respectively.

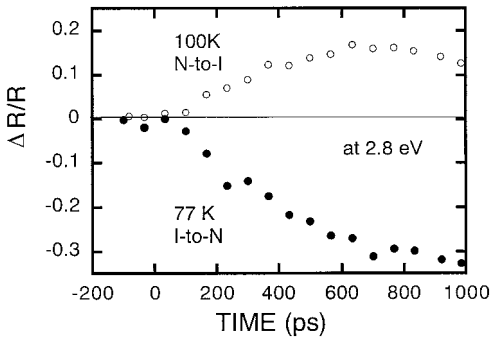

Figure 8. Time profiles of the PR signals observed at 2.8 eV induced by the irradiation of 1.55-eV light pulse with 80-fs pulse width. Results observed at 77 K (conversion from I-phase to N-phase) and 100 K (N-to-I conversion) are plotted by closed and open circles. The photon flux for excitation was 1×10^{14} cm^2.

I-phase and N-phase crystals were photoconverted into metastable N- and I-phases. Such a large photoresponse is considered to be due to degeneracy in the energy levels of the N- and I-phases as a result of cooperative interaction inside the crystals. More detailed data on the excitation intensity dependence of the photoconverted fraction will be shown in the next chapter, and a discussion on the role of cooperative CT interaction will be given in chapter VI.

To measure the speed of the phase conversion, a time-resolved study was carried out. The time profiles of the PR signals observed at 2.8 eV are plotted in Figure 8. As shown in Figure 7a, negative and positive PR signals are observed for I-to-N

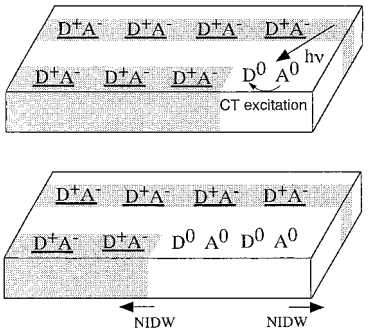

Figure 9. Schematic view graph of the growth process of the metastable N-phase domain from the localized CT excited state in the host I-phase crystal. As can be observed, the generation and movement of the domain wall connecting N- and I-phase domains (NIDW) can be triggered by the photoinjected localized species.

and N-to-I phase conversions, respectively, at this photon energy. As expected, the PR signals remain either negative (at 77 K) or positive (at 100 K) over the whole time domain. As shown in Figures 7 and 8, the PR signals start to increase at $\Delta t = 100$ ps and are gradually enhanced until they reach their optimum value at around $\Delta t = 700$ ps. These results observed at 77 K (100 K) indicate that local excited species injected by an 80-fs laser pulse into the host I-phase (N-phase) crystal grow into the macroscopic N-phase (I-phase) domain within a period of 1 ns, as schematically shown in Figure 9.

The excitation intensity for this experiment was 1×10^{14} cm^{-2}. The dynamics of the phase conversion strongly depends on the excitation intensity. This issue will be discussed at length in the latter part of the next chapter.

Not only the intensity but also the spectral shape of the PR signal seem to change as the delay time (Δt) increases in the dynamical process of the PIPT. For example, at 77 K, PR peaks observed around 3.0 eV well after excitation ($\Delta t = 670$ ps) seem to be located at higher photon energy sides immediately after excitation ($\Delta t = 300$ ps). Lattice structural changes accompanied with a change in the ionicity (ρ) of constituent molecules are possibly the origin of the "shape-up" process observed in the temporal changes of the PR spectra. At the present stage, the mechanism is not clear, and PR spectra measurements in a much wider photon energy region ($h\nu = 0.1-10$ eV) are necessary for further discussion.

The observed PR signals were transient and disappeared within 1 ms. In other words, the photoinjected phase domain by 80-fs pulsed-light irradiation was metastable. The metastability of the photoinjected domain was also reported by use of pulsed laser excitation with widths of 20 ns and 60 ps.[3,21] The reason for the transience of the photosignal observed in TTF-CA crystals remains to be determined. It could tentatively be said that TTF-CA crystals show a first-order phase transition; however, the hysteresis has a very narrow width (nearly zero). This means that the height of the potential barrier between the stable and metastable phases, i.e., the N- and I-phases, is rather low around T_c, as discussed above (see Figure 2). In such a case, the metastable phase domain can easily go back to the original stable one by thermal excitation (see Figure 2a,b) and, as a result, the photoinduced effect results in a transient, not a permanent, PIPT.[9]

It could be suspected that the observed PR signal originates in the accumulation of the photoexcited species due to the rather high repetition rate (1 kHz) of an excitation laser pulse. However, such a deceptive effect can easily be disregarded, since no PR signal was observed when the monitor light pulse irradiated 100 ps before the excitation pulse (see Figure 7b,c).

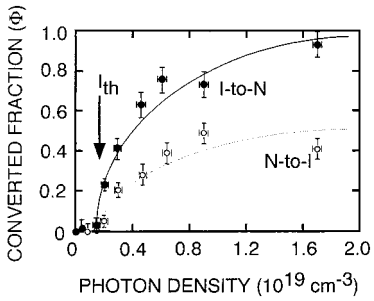

Figure 10. Excitation intensity dependences of the photoconverted fractions (Φ) for I-to-N (closed circles) and N-to-I (open circles) PIPT. Solid and dotted lines are viewing guides. The arrow and I_{th} denote the threshold intensity for excitation.

In other words, the PR signal became very small 1 ms after excitation. In addition, basically the same PR signal was observed when the repetition rate of the excitation pulsed light was decreased to less than 50 Hz.

V. Characteristics of N−I PIPT in TTF-CA

As discussed in the first chapter, the photoresponse of crystals that show a phase transition due to cooperative interaction will be quite different from the ordinal case. In crystals in which cooperative interaction is very weak, the photoexcited species will be localized around the excited molecules. Thus, the photoresponse will increase parallel to the increase in excitation intensity (see solid line in Figure 3). In contrast, the appearance of a threshold-like behavior in the excitation intensity dependence of the magnitude of the photoresponse can be expected for crystals with rather strong cooperative interaction (see dashed line in Figure 3). Here, we report the excitation intensity dependences of the converted fractions (Φ) for I-to-N and N-to-I PIPTs. We demonstrate that threshold-like behavior, i.e., a photoswitching effect, is seen in TTF-CA crystals in which cooperative CT interaction plays a key role for their exotic natures. In addition, we also report that the dynamical behavior of the I-to-N PIPT strongly depends on the excitation intensity.

In Figure 10, the excitation intensity dependences of the photoconverted fractions (Φ) for I-to-N and N-to-I PIPT are plotted by closed and open circles. The PR signal in the photon energy region between 2.15 and 2.35 eV observed at $\Delta t = 870$ ps was integrated, and Φ was estimated by comparing the integrated intensity of PR with that of the calculated differential one. Similar Φ values were obtained even if they were estimated on the basis of the PR signals observed at 2.9 eV. In addition, the excitation photon density (photons/cm^3; hereafter abbreviated as cm^{-3}) was estimated as follows: the attenuation depth for visible and near-UV-region light is about 100 nm for the vacuum-deposited film of TTF-CA. The total excitation photon flux was roughly assumed to be homogeneously absorbed in the crystal surface region with a depth of 100 nm. On this assumption, for example, the excitation light intensity with a photon flux of 5×10^{13} (4×10^{13}) photons/cm^2 that was used for measuring the PR spectra at 77 K (100 K), as shown in Figure 7, corresponds to a photoexcitation density of 5×10^{18} (4×10^{18}) cm^{-3}.

The first important feature of the plot in Figure 10 is that Φ increases abruptly if the excitation photon density becomes higher than 2×10^{18} cm^{-3}, which is indicated by an arrow and noted as I_{th}. Threshold-like behavior is a common characteristic for I-to-N and N-to-I conversion, both shown by closed and open circles, respectively. As discussed previously, a nonlinear dependence of Φ on the excitation intensity can be expected

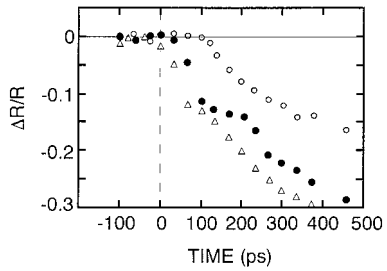

Figure 11. Time dependence of the PR signal observed at 3.0 eV with various excitation intensities. Open circles, closed circles, and triangles are for excitation intensities of 2×10^{18}, 9×10^{18}, and 1.7×10^{19} cm^{-3}, respectively. The sample temperature was 77 K, and the crystal was in the I-phase before excitation by 1.55-eV light pulse.

for crystals with strong cooperative interaction. It can be concluded that the observed results reflect the importance of cooperative CT interaction in the driving process of this exotic photoeffect, i.e., N−I PIPT.

The second notable point of Figure 10 is high photoconversion efficiency. For example, 75% and 35% of the crystal surface is subject to I-to-N and N-to-I conversion with a photoexcitation density of 6×10^{18} cm^{-3}, as plotted by closed and open circles, respectively. The density of DA pairs in TTF-CA crystals is 2.46×10^{21} cm^{-3}, and the estimated excitation density thus corresponds to one excitation photon for every 410 DA pairs.[12] Therefore, that single excitation photon changes the $410 \times 0.75 = 310$ ($410 \times 0.35 = 140$) DA pairs from ionic to neutral (neutral to ionic). In addition, the threshold intensity (I_{th}), 1.7×10^{18} cm^{-3}, corresponds to that single excitation photon for every 1400 DA pairs. Such a large photoresponse is considered to be due to the degeneracy in the energy levels of N- and I-phases by virtue of cooperative interaction inside the crystals. In such cases, the concept of neutral−ionic domain wall (NIDW), i.e., a microscopic interface separating the N domain from the I domain, is useful to describe the photoelectronic process. Subsequently, a number of experimental results consistent with the concept of NIDWs has been found in TTF-CA and other DA solids near the N−I phase boundary.[18,20,22] In this sense, the presently observed N−I PIPT can be interpreted in terms of the photodoping of NIDWs, as shown in Figure 9. The theoretical aspects of NIDW will be discussed in chapter VI.

Even when the repetition rate of the excitation pulsed light was decreased to 50 Hz, no significant changes were observed in the excitation-intensity dependence of the converted fraction Φ and the dynamical behavior of the PR signal. Therefore, we concluded that the observed threshold-like behavior is not an artificial effect induced by the accumulation of photoexcited species. Experiments using the laser system with repetition rates lower than 10 Hz would be necessary for a more accurate study.

Not only the photoconverted fraction (Φ) but also the dynamics of the phase conversion strongly depend on excitation photon density. Figure 11 shows the time dependence of the PR signal observed with various excitation intensities. With rather weak photoexcitation, the PR signal starts to increase 100 ps after the irradiation of the light pulse. However, with high intensity, the PR signal begins to increase immediately after excitation. Careful checks have shown that the observed result is not an artificial effect due to the misalignment of the excitation and monitor lights. The observed time delay in the PR signals to the excitation pulse is analogous to the "incubation time" reported for martensitic transformations.[23]

These findings strongly support the idea that cooperative CT interaction plays an essential role in the dynamics of N−I PIPT. In addition, it has recently been reported that the threshold intensity (I_{th}) for Φ increases when the excitation photon energy is nearly resonant to the CT excitation between constituent TTF and CA molecules.[24] This result, which was obtained using a wavelength tunable nanosecond pulsed laser system, also suggests that the dynamical process from the localized CT excited state to the metastable phase domain strongly depends on excitation photon energy. This idea is currently tentative, and studies using a wavelength tunable femtosecond laser system would be necessary for further discussion.

VI. Theoretical Considerations on the N−I PIPT

The PIPT phenomenon has not been thoroughly studied from a theoretical point of view yet. There are, however, pioneering papers[7] that have addressed the problem. There are many interesting aspects of the phenomena, such as nonlinear relaxed excitations,[25] mechanisms of lattice relaxation,[26] and the dynamics of the formation of photogenerated domains. Within the simplest two-diabatic state model, different mechanisms have been shown for one-dimensional[27] (nucleation picture) and three-dimensional processes. The usefulness of mean-filed approximation has been also shown when the process is being modeled by Ising spin Hamiltonian.[28] Furthermore, a detailed analysis of the dynamics of the photoinduced structural changes under adiabatic approximation has recently been presented as an extension of earlier studies.[29] It has to be stressed that the term "photoinduced structural changes" is used instead of PIPT strictly when one-dimensional systems are considered. The above-mentioned research should be used as a guide in constructing a model for N−I PIPT. The critical requirement for a model of PIPT is that it give a picture that is consistent with our present understanding of the temperature- and pressure-induced N−I transition.[30] Thus, reference will be made to earlier studies on the thermodynamics of the transition and, in particular, to the model of condensation and crystallization of CT excitations.[30−32]

When constructing a model, it is important to take advantage of the fact that CT organic compounds are quasi-one-dimensional crystals and, in particular, that the mixed-stack architecture with alternating D and A molecules stimulates electron transfer along the chain. Taking into account the electronic-structural aspects, the system can be approximated as a set of weakly interacting stacks. Stacks, on the other hand, are one-dimensional systems with strong electron−electron and electron−phonon couplings.

Our model is based on the diabatic energy functions for two states, corresponding to N and I structures. First, we constructed the diabatic function for the N stack. Following experimental evidence and the model for the N−I transition in TTF-CA crystal,[30] we deduced that the valence electrons that are subject to intermolecular transfer are strongly coupled to a dimerization mode. The normal coordinate of the mode will, therefore, be a convenient structural variable for diabatic energy functions. For the purpose of our model, assuming a reference zero energy for a stack of N molecules, the diabatic state is expressed in terms of the dimerization mode displacement, u, and frequency, ω_N,

$$E^N(u) = {}^1/_2\omega_N{}^2u^2 + {}^1/_4cu^4 \quad (1)$$

The mixed stack of N molecules is stable ($\omega_N > 0$, $c > 0$), and the diabatic state forms a single well potential, indicated as E^N in Figure 12a.

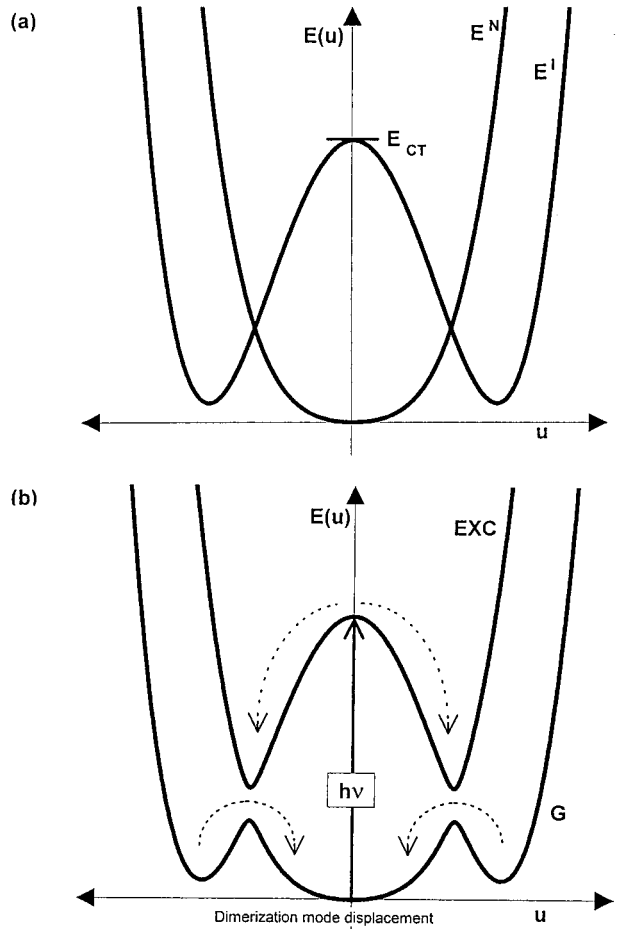

Figure 12. (a) (Free) energy functions for diabatic states corresponding to N (eq 1) and I (eq 3) phases in the TTF-CA crystal. (b) Adiabatic ground (G) and excited (EXC) states, formed by the quantum mixing of the diabatic states shown in (a).

Next, we constructed the diabatic function for a domain of I molecules. Such a stack has important features which have to be taken into account. First, there is equal probability for an electron transfer from D to the nearest left and right A molecule, and this creates degeneracy of the CT state in the mixed stack. Moreover, strong electron−electron coupling and the one-dimensionality of the stack stimulate a formation of CT excitonic strings,[33] the collective excitations that are bound states of more than two CT excitons (D^+A^- or A^-D^+ pairs). States $|...DA(D^+A^-)_nDA...\rangle$ and $|...DAD(A^-D^+)_nA...\rangle$ have equal energies, separated by the energy of $E_{CT}(n)$ from the neutral state, $|...DA(DA)_nDA...\rangle$, as shown in Figure 13. A symmetric (A_g) and antisymmetric (A_u) combination of the CT strings creates CT states, which are accessible by the two-photon process and one-photon absorption, respectively. As long as the quantum mixing of the ionic and neutral states is neglected (the diabatic approximation), the energies of the CT states are equal. The energy expense to ionize a string of *n*-DA pairs is,[33,34]

$$E_{CT}(n) = n(I-A) - M(n)J \quad \text{and} \quad E_{CT}(1) = I - A - J \quad (2)$$

where I is the ionization energy of the D molecule, A is the electron affinity of A molecules, and $M(n)J$ is the Coulomb energy of the string expressed in terms of the Madelung constant, $M(n)$. The important feature of the string is that its energy follows from a balance between the energy needed to ionize molecules (linear on n) and the gain due to the Coulomb interaction (nonlinear on n). This balance, as has already been

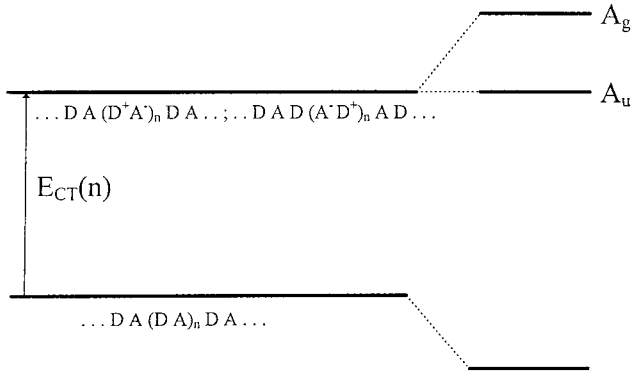

Figure 13. Scheme of energy levels for CT strings without lattice relaxation. The right-hand side diagram follows from the mixing of the CT states.

pointed out, has been at the heart of the concept of N−I transition for many years.[10] The strong electron−electron interaction along the stack creates cooperativity and decreases the energy cost for the ionization of DA pairs in the neighborhood of the string, bringing the ionized pairs together. This is the essence of the formation of the CT excitonic strings.[33] Cooperativity substantially increases by strong electron−phonon coupling, causing a "domino effect."[29]

To construct a diabatic state energy function for a lattice-relaxed I stack, we have to consider a considerable energy gain due to the strong coupling between the transferred electron and the dimerization mode. Asking how the lattice relaxation process takes place may not be immaterial, since for the case at hand, the electron−electron coupling may compete for priority with the electron−phonon coupling. In other words, does the formation of a lattice-relaxed CT string proceed via the creation and posterior relaxation of a CT string or as a clustering of lattice-relaxed pairs of ionized molecules? Hanamura provides a strong argument for the first mechanism:[27] the effective mass of the CT string (exponentially increasing with n) is so large that it guarantees the localization of the excitation, which is required for lattice relaxation. This means that larger CT strings have better chances to create lattice-relaxed states that will not decay radiatively. It should be stressed that this mechanism is different from that of a polaron formation. The usual polaron problem involves a single electron coupled to a deformable medium. The novelty of CT complexes is the occurrence of self-trapping at rather high concentrations of the transferred electrons. Therefore, the diabatic state should be constructed for a string of ionized molecules above some critical size so that it is able to create metastable or stable states.

Strong electron−phonon interaction stabilizes the *n*-CT string by energy gain (CT reorganization energy) due to additional electrostatic and elastic (intramolecular, totally symmetric deformations) interaction between the I molecules. The A_u CT exciton string couples to the dimerization mode (A_u symmetry), and the interaction destabilizes the undimerized stack. Due to the polar degeneracy of the A_u excitonic string, the diabatic state for the string of I molecules will be in the form of double-well potential,

$$E^I(n,u) = (1/n)\,E_{CT}(n) + {}^1/_2\omega_N{}^2(1-\chi)u^2 + {}^1/_4c'u^4 \ (\chi > 1, c' > 0) \quad (3)$$

with parameters as already defined. The instability index, χ (which depends on the size of the string), shows how long-range Coulomb and elastic interactions destabilize the mixed stack along the pattern of the dimerization mode. For pure

Coulomb interaction, the index has been calculated,[35] showing that an alternating stack of ionized molecules is highly unstable against dimerization distortion. The minima of the diabatic potential for the I string correspond to double degenerate states of the lattice-relaxed CT string (see Figure 12a). It should be noticed that function $E^{I}(\infty,u)$ corresponds to the diabatic energy for the I stack, in complete analogy to the well-known case of polyacetylene.[19]

The N−I transformation in the single mixed stack is discussed within the model of diabatic states, which is valid when quantum mixing of the states is small (long strings). The diabatic states, considered to be energy states, may be treated as free energy states assuming that the functions drawn in Figure 12 are integrated over all lattice variables except the dimerization mode displacement, which behaves as a transformation path. It is advantageous to see the states as free energy states, as it facilitates the relation to the theory of electron-transfer reaction.[36]

The illumination of a stack of N molecules (higher-temperature phase) with energy higher than $E_{CT}(1)$ excites the A_u CT exciton by one-photon absorption (and possibly the A_g CT exciton via two-photon absorption). Due to electron−electron coupling, the A_u exciton grows into a CT string in a rather quick process. In the next step, due to localization and strong electron−phonon coupling, it relaxes into a dimerized string, with equal probability of "right" and "left" polarized domains. The one-dimensional domains of the lattice-relaxed CT strings are metastable when the size of the strings is larger than a critical value typical for the nucleation and growth mechanism of the one-dimensional system. The domains exist even after the illumination of the crystal is switched off, decaying slowly afterward by thermal relaxation.

Strictly speaking, thermal relaxation requires an adiabatic rather than a diabatic picture. Let us take into account a quantum mixing of the N and I strings. The coupling is due to the overlap of HOMO and LUMO orbitals of D and A molecules, respectively. For a quantum mixing of strings, the overlap integral can be approximated as $t(n) \cong t^n(1)$, which is relatively small ($t(1) < 1$ eV) for most CT complexes, including TTF-CA. The diabatic state picture is slightly modified. The mixing forms adiabatic ground and excited CT states, as shown in Figure 12b. A characteristic feature of the ground state is that it has three minima, a clear indication of (cooperative) multistability. In addition, the ionicity of the molecules (q) in the state strongly depends on the size of the string and the displacement, $q(n,u) = {}^1/_2[1 - \Delta/(\Delta^2 + 4t^2)^{1/2}]$, where $\Delta = E^{I} - E^{N}$ and t depends on both n and u. In the undimerized stack, the mixing is such that $q_N \cong 0.3$ for (quasi-) N molecules. Due to quantum mixing, the path for the relaxation of the A_u CT string changes slightly. At first, after the formation of the string, it relaxes along the path of the excited state toward its energy minima, and the dynamics of this relaxation process can be described by the energy function of the excited state. At the minima in the excited state, these partially relaxed CT strings are absolutely unstable and relax further into the ground state as they emit energy, still having higher energy than any stable or metastable configurations in ground states. The next process is relaxation along the ground state energy profile into a metastable or stable minimum, depending on which side of the barrier the system has relaxed onto from the excited state. It is thus evident that details of the energy functions are extremely important for the mechanism of N−I structural changes.

The photoinjected metastable phase of the lattice-relaxed CT strings can be visualized as a disordered stack of oppositely polarized strings (ionic domains). These strings relax thermally into a more stable N chain, overcoming the energy barrier (activation energy), as indicated by dashed arrows in Figures 2 and 12b. Thermal mixing of the domains corresponds to thermal tunneling between the minima of the ground state and is proportional to $\exp(-E_{DW}/kT)$,[37] where E_{DW} is the energy of NIDW. The thermal relaxation of the metastable I strings into the N-phase can be seen as a motion of the NIDWs (see Figure 9). Within this picture, it might be conceived that photoinduction of the I-phase from N is at the expense of the energy of NIDW. In other words, the discussed photoinduced phenomenon corresponds to an "injection" of NIDW, which might play a role in elementary excitations.[37]

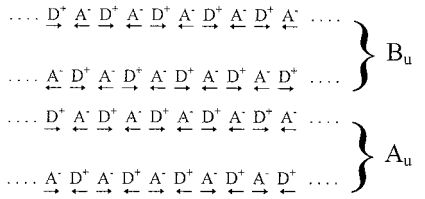

Figure 14. Illustration of the dimerization pattern (indicated by arrows) of A_u and B_u modes for two interacting and translationally nonequivalent chains in the TTF-CA crystal.

Thermal mixing eliminates the degeneracy of the "right" and "left" polarized strings and, for symmetry, TTF-CA crystal favors the antisymmetric combination of the strings, e.g., the polar structure of a stack. Thus, when the CT strings on a single stack of D and A molecules relax structurally, there will be a slightly higher probability that they will form domains of a polar rather than nonpolar structure. These polar and nonpolar phases of the lattice-relaxed CT strings of a single stack are considered to act as precursors of the thermodynamically stable phases found in TTF-CA, called I_{ferro} and I_{para}, respectively.[30]

Next, it is necessary to discuss the influence of interstack couplings. In TTF-CA crystal, there are two complex units in the primitive unit cell. This means that there are two nonequivalent (related by 2-fold axis) stacks in the crystal, which create two polar CT string states, A_u, with opposite polarity of strings on the neighboring stacks, and B_u, with parallel polarity of the stacks, as shown schematically in Figure 14. Clearly, the dimerization modes are also of A_u and B_u symmetries, and linear coupling requires the same symmetries for the excitations. The energy difference between the modes is the nonequivalence of the stacks. It is expected to be very small and not strong enough to discriminate energetically the relaxed strings of these two symmetries.

The interstack coupling, expected to be much smaller than that within stacks, can be conveniently treated within the parameters of mean-field approximation. In the approximation, the surrounding stacks generate a field, which couples to the polar and nonpolar structures of the lattice-relaxed excitonic strings created within two nonequivalent stacks. It could be assumed that the diabatic (adiabatic) free energy state corresponding to the ionic structure in Figure 12 represents now the state for lattice-relaxed CT strings of B_u symmetry. The reason is that the thermodynamically stable I-phase of TTF-CA with symmetry Pn,[31] observed in a low-temperature, low-pressure region,[30] might be considered as the N-phase deformed according to the pattern of the B_u mode. The minima of the (free) energy curve in Figure 12b would correspond to ferroelectric domains with opposite polarization. The mean field of the surrounding stacks couples to the states, decreasing their energies. Qualitatively, it seems that the picture of relaxation of the CT strings after photoinduction does not change when

the interstack coupling is included. However, this mean field will play a key role in the observed threshold behavior.[28]

On concluding this chapter, we stress that the present model, based on diabatic energy functions, is an important foundation for a statistical, spin-1 lattice-gas model. By means of assignments $S = \pm 1$ for the ferroelectric domains of a chain and $S = 0$ for a paraelectric one, the model has been used to interpret the thermodynamics of the N−I transition.[30,32] The mechanism of photoinduced ferroelectricity, which is the essence of N−I PIPT, will therefore be well described by nonequilibrium properties (switching phenomena) of the spin-1 lattice-gas model. It has been shown that the minimum version of the model (Blume−Capel model) may be used to describe a possible mechanism for photoinduced ferromagnetism.[38] In addition, on the base of the present model, the dynamics of the N−I PIPT could be analyzed within a phenomenological relaxation equation. The equation describes the relaxation of the dimerization order parameter, u, after a change in concentration of relaxed I pairs due to illumination. This might be described as follows,

$$du/dt = -k[a(T - T_c) + \alpha c']u + bu^3 + cu^5 \qquad (4)$$

where a, b, and c are coefficients of the (free) energy expansion describing the potential with three minima. c' is the concentration of ionic dimers, coupled to polarization (parameter α). The concentration is governed by a kinetic equation that takes into account a competition between optical pumping and thermal relaxation.[28] An analysis of the obtained experimental results based on this phenomenological model is now in progress.

VII. Summary

This is the first study to report that cooperative charge transfer among constructive molecules (N−I PIPT) can be induced in TTF-CA crystals by irradiation with an 80-fs laser pulse. We have demonstrated that N−I PIPT is bidirectional and that the photoinjected localized excited states grow into the macroscopic metastable phase domain within 1 ns. The excitation intensity dependences of the photoconverted fraction (Φ) and the growth dynamics from the localized photoexcited species into the macroscopic domain show the threshold-like behavior characteristic of photoinduced cooperative phenomena. On the basis of various experimental results, the importance of cooperative CT interaction in the driving process of PIPT is discussed from the theoretical viewpoint.

As shown in this work, recent advancements in both the femtosecond laser technique and the knowledge of cooperative phenomena in condensed matters have unveiled new aspects of the CT effect in solids that are attractive targets for both chemistry and physics. We strongly believe that further studies on this system by means of tunable femtosecond laser techniques will additionally make it possible to control various cooperative phenomena such as magnetic, dielectric, and structural transitions in molecular crystals by photoexcitation.

Acknowledgment. The authors would like to thank Professor Takao Koda, Professor Fujio Minami, and Professor Herve Cailleau for enlightening discussions and Dr. Sachio Horiuchi (JRCAT) for making the resistivity data available. This work was partially supported by the Nissan Scientific Foundation and a Grant-in-Aid for Scientific Research from the Ministry of Education, Science, Sports, and Culture, Japan. T.L. acknowledges the hospitality of Professor Herve Cailleau and the Groupe Matiere Condensee et Materiaux, Universite de Rennes, as well as the support for Polish-Japanese cooperation from the Committee for Scientific Research, Poland.

References and Notes

(1) Koshihara, S.; Tokura, Y.; Takeda, K.; Koda, T. *Phys. Rev. Lett.* **1992**, *68*, 1148.

(2) Kawanishi, Y.; Tamaki, T.; Seki, T.; Sakuragi, M.; Ichimura, K. *Mol. Cryst. Liq. Cryst.* **1992**, *218*, 153.

(3) Koshihara, S.; Tokura, Y.; Mitani, T.; Saito, G.; Koda, T. *Phys. Rev.* **1990**, *B42*, 6853.

(4) Sekine, A.; Tatsuki, H.; Ohashi, Y. *Mol. Cryst. Liq. Cryst.* **1994**, *242*, 109.

(5) Koshihara, S.; Tokura, Y.; Iwasa, Y.; Koda, T. *Phys. Rev.* **1991**, *B44*, 431.

(6) Tanaka, T.; Miyano, K.; Tomioka, Y.; Tokura, Y. *Phys. Rev. Lett.* **1997**, *78*, 4257.

(7) *Relaxation of Excited States and Photoinduced Structural Phase Transitions*; Nasu, K., Ed.; Springer Series in Solid-State Science, 124; Springer: Berlin, 1997.

(8) Koshihara, S.; Tokura, Y.; Takeda, K.; Koda, T. *Phys. Rev.* **1995**, *B52*, 6265.

(9) Koshihara, S. In *Optical Properties of Low-Dimensional Materials 2*; Ogawa, T., Kanemitsu, Y., Eds.; World Scientific: Singapore, 1998; Chapter 3.

(10) Torrance, J. B.; Vanzquez, J. E.; Mayerle, J. J.; Lee, V. Y. *Phys. Rev. Lett.* **1981**, *46*, 253. Torrance, J. B.; Girlando, A.; Mayerle, J. J.; Crowley, J. I.; Lee, V. Y.; Batail, P. *Phys. Rev. Lett.* **1981**, *47*, 1747.

(11) Tokura, Y.; Koda, T.; Mitani, T.; Saito, G. *Solid State Commun.* **1982**, *43*, 757.

(12) Kanai, Y.; Tani, M.; Kagoshima, S.; Tokura, Y.; Koda, T. *Synth. Met.* **1984**, *10*, 157.

(13) Tokura, Y.; Kaneko, Y.; Okamoto, H.; Tanuma, S.; Koda, T.; Mitani, T.; Saito, G. *Mol. Cryst. Liq. Cryst*. **1985**, *125*, 71.

(14) Girlando, A.; Zanon, I.; Bozio, R.; Pecile, C. *J. Chem. Phys.* **1978**, *68*, 22.

(15) Le Cointe, M.; Lemee-Cailleau, M. H.; Cailleau, H.; Toudic, B.; Toupet, L.; Heger, G.; Moussa, F.; Schweiss, P.; Kraft, K. H.; Karl, N. *Phys. Rev.* **1995**, *B51*, 3374.

(16) Torrance, J. B. In *Low-Dimensional Conductors and Superconductors*; Jerome, D., Caron, L. G., Eds.; NATO ASI Series B155; Plenum: New York, 1987.

(17) Nagaosa, N.; Takimoto, J. *J. Phys. Soc. Jpn.* **1986**, *55*, 2735.

(18) Okamoto, H.; Mitani, T.; Tokura, Y.; Koshihara, S.; Komatsu, T.; Iwasa, Y.; Koda, T. *Phys. Rev.* **1991**, *B 43*, 8224.

(19) *Electronic Properties of Conjugated Polymers III*; Kuzmany, H. K., Mehring, M., Roth, S., Eds.; Springer Series in Solid-State Sciences 91; Springer-Verlag: Berlin, 1989.

(20) Mitani, T.; Saito, G.; Tokura, Y.; Koda, T. *Phys. Rev. Lett.* **1984**, *53*, 842.

(21) Koshihara, S.; Tokura, Y.; Sarukura, N.; Segawa, Y.; Koda, T.; Takeda, K. *Synth. Met.* **1995**, *70*, 1225.

(22) Tokura, Y.; Okamoto, H.; Koda, T.; Mitani, T.; Saito, G. *Physica* **1986**, *143B*, 527. Mitani, T.; Kaneko, Y.; Tanuma, S.; Tokura, Y.; Koda, T.; Saito, G. *Phys. Rev.* **1987**, *B35*, 427. Mitani, T.; Tokura, Y.; Kaneko, Y.; Takaoka, K.; Koda, T.; Saito, G. *Synth. Met.* **1987**, *19*, 515. Tokura, Y.; Okamoto, H.; Koda, T.; Mitani, T.; Saito, G. *Phys. Rev.* **1988**, *B38*, 2215.

(23) Kakeshita, T.; Fukuda, T.; Saburi, T. *Scr. Mater.* **1996**, *34*, 147.

(24) Suzuki, T.; Sakamaki, T.; Tanimura, K.; Koshihara, S.; Tokura, Y. To be published.

(25) Nasu, K. In ref 7.

(26) Toyozawa, Y. In ref 7.

(27) Hanamura, E.; Nagaosa, N. *J. Phys. Soc. Jpn.* **1987**, *56*, 2080. Nagai, T.; Nagaosa, N.; Hanamura, E. *J. Luminescence* **1987**, *38*, 314. Hanamura, E. In ref 7.

(28) Nagaosa, N.; Ogawa, T. *Phys. Rev.* **1989**, *B39*, 4472. Ogawa, T.; Nagaosa, N. In ref 7.

(29) Koshino, K.; Ogawa, T. *J. Phys. Soc. Jpn.* **1998**, *67*, 2174.

(30) Lemee-Cailleau, M. H.; Le Cointe, M.; Cailleau, H.; Luty, T.; Moussa, F.; Ross, J.; Brinkmann, D.; Toudic, B.; Ayache, C.; Karl, N. *Phys. Rev. Lett.* **1997**, *79*, 1690.

(31) Cailleau, H.; Le Cointe, M.; Lemee-Cailleau, M. H. In ref 7.

(32) Luty, T. In ref 7.

(33) Kuwata-Gonokami, M.; Peyghambarian, N.; Meissner, K.; Flugel, B.; Sato, Y.; Ema, K.; Shimano, R.; Mazumdar, S.; Guo, F.; Tokihiro, T.; Ezaki, H.; Hanamura, E. *Nature* **1994**, *367*, 47.

(34) Luty, T. *Acta Phys. Polon.* **1995**, *A87*, 1009.

(35) Iizuka-Sakano, T.; Toyozawa, Y. *J. Phys. Soc. Jpn.* **1996**, *65*, 671.

(36) Marcus, R. A. *Annu. Rev. Phys. Chem.* **1964**, *15*, 155. Marcus, R. A.; Sutin, N. *Biochim. Biophys. Acta* **1985**, *811*, 265.

(37) Nagaosa, N. *J. Phys. Soc. Jpn.* **1986**, *55*, 3488.

(38) Nishino, M.; Yamaguchi, K.; Miyashita, S. *Phys. Rev.* **1998**, *B58*, 9303.